RevMexAA (Serie de Conferencias), **13**, 170–176 (2002)

BUBBLES, BOW-SHOCKS, AND BULLETS OVER BROAD-LINES: THREE IONIZED OUTFLOWS RESOLVED WITH *HST*

G. Cecil,[1] P. Ferruit,[2], and S. Veilleux[3]

RESUMEN

Las imágenes y espectros de flujos de alta velocidad de AGNs (núcleos activos de galaxias) obtenidos con el *HST* logran: (1) Mostrar sistemas de choque a proa/disco de Mach de tamaños de $\sim 5''$ en las puntas del radio jet de NGC 4258. Argumentamos que el jet ha precesado a su orientación corriente observada a escalas de VLBI. (2) Resolver los perfiles de las líneas de [O III] 5007 Å y Hβ en la NLR de NGC 1068, y mostrar nudos compactos corridos al azul a velocidades >3100 km s^{-1} relativas al gas ambiente. Los nudos están a varios arcosegundos afuera del núcleo, sobre y fuera del radio jet, y son cinemáticamente cercanos a nubes más brillantes que se mueven a 200–800 km s^{-1} (respecto a la velocidad sistémica). Argumentamos que los nudos corresponden a material ablacionado de nubes masivas por el jet y que este material está siendo acelerado por la presión de radiación. Estos nudos son buenos candidatos para los "absorbedores UV intrínsecos" observados en otros AGN. (3) Resolver muchos de los filamentos que forman la superburbuja (de 1 kpc de diámetro) de NGC 3079. Combinando estas imágenes con observaciones terrestres de Fabry-Perot, obtenemos límites para las densidades, factores de llenado y velocidades espaciales, de forma que limitamos la masa total de gas ionizado, su momento y la energía cinética de este flujo poco colimado. Los perfiles de emisión más anchos están en la base de la superburbuja, y coinciden con el eje del jet de escala VLBI. Por otro lado, dada su similitud a simulaciones hidrodinámicas y por su configuración de campo magnético, la mayor parte de la super burbuja parece haber sido inflada por un viento nuclear con una luminosidad mecánica de 10^{43} erg s^{-1}.

ABSTRACT

HST images and spectra of high-velocity outflows from three AGN: (1) Show 5″-long bow shock/Mach disk complexes at the ends of the active radio jet in NGC 4258. We argue that the jet has precessed to its current orientation seen at VLBI-scales. (2) Fully resolve [O III] 5007 Å and Hβ line profiles in the NLR of NGC 1068, and show compact knots with blueshifted radial velocities >3100 km s^{-1} relative to ambient gas. The knots lie several arcseconds outside the nucleus, on and away from the radio jet, and are kinematically contiguous with brighter clouds moving 200–800 km s^{-1} relative to systemic. We argue that the knots are ablata streams undergoing radiative acceleration from jet-agitated, massive clouds. They are good candidates for "intrinsic UV absorbers" seen in other AGN. (3) Resolve many of the filaments that form the 1 kpc-diameter superbubble of NGC 3079. Combining with ground-based Fabry-Perot spectra, we constrain gas densities, gas filling factors, and space velocities, thereby bounding the total ionized mass, momentum, and KE of this wide-angle outflow. The broadest emission line profiles lie at the base of the superbubble, and coincide with the axis of the VLBI-scale jet. However, the bulk of the superbubble, by its resemblance to hydro simulations and by its pattern of magnetic fields, appears to be inflated by a nuclear wind of mechanical luminosity 10^{43} erg s^{-1}.

Key Words: **GALAXIES: ACTIVE — GALAXIES: JETS — GALAXIES: KINEMATICS AND DYNAMICS — HYDRODYNAMICS — ISM: JETS AND OUTFLOWS**

Emission Lines from Jet Flows (Isla Mujeres, Q.R., México, November 13-17, 2000)
Editors: W. J. Henney, W. Steffen, A. C. Raga, & L. Binette

1. INTRODUCTION

Throughout this conference, just beyond the rumble of the air-conditioners, one can almost hear the chorus of theorists chanting "weather, weather, ...". Yet the mode and history of cloud acceleration (direction, duty cycle, constituent particles) are the only parts of the theorists' toy models that we can constrain by observation, so are the subjects of this conference. To address these hard topics, one can search for patterns as functions of redshift, host environment, and nuclear bolometric luminosity; several summaries are given in these proceedings. We can also study select prototypes in detail, assembling the multi-frequency datasets needed to track an outflow as it interacts with various phases of the galaxy ISM.

Our group has followed the second track, and Veilleux et al. (2002) is an update on our survey of nearby AGN. Often, outflows extend to arcminute scales in our targets, but energetic regions are dis-

[1]Dept. of Physics & Astronomy, U. North Carolina, USA.
[2]Observatoire de Lyon, France.
[3]Dept. of Astronomy, U. Maryland, USA.

Emission Lines from Jet Flows (Isla Mujeres, Q.R., México, November 13-17, 2000)
Editors: W. J. Henney, W. Steffen, A. C. Raga, & L. Binette

tributed sparsely across this field. We have therefore exploited the efficiency of Fabry-Perot (FP) spectrometers to increase contrast and to map the full extent of the optically emitting outflow. In this way we avoid biased slit placements on complex targets, but these spectrometers limit us to a few emission lines, primarily [O III] 5007 Å, [N II], and Hα. As I discuss in Cecil (2000a), symmetries in flux, radial velocity, and dispersion images motivate kinematical models to reconstruct the missing dimensions of phase space; only then can we address flow energetics. Where we find symmetries, we constrain dynamics and publish; Veilleux et al. (2002) list the papers in their Table 1. With models to test, we next place long-slits for other spectral constraints at strategic locations.

Often, target structures are compact and may attain highest spectral constrast in the UV. If our proposed targets are notorious enough to be known by TAC members, we can use *HST* to tighten dynamical constraints. Its imagers can resolve filaments, and STIS can obtain spectra of the brightest, least dusty clumps. In §§ 2 and 3 we summarize two of our recently published studies on outflows which combine ground-based imaging spectra with *HST* WFPC2 filter imaging. In § 4 we present preliminary results from STIS spectra on a third.

2. NGC 3079: ROLE OF THE JET IN A WIDE-ANGLE OUTFLOW

NGC 3079 is a nearly edge-on spiral galaxy at 17.5 Mpc. An X-shaped structure around the nucleus was resolved into a figure-8 shell pattern (Duric & Seaquist 1988), and was shown (Ford et al. 1986) to contain a bubble of optical line-emission that extends from the nucleus to 1.2 kpc above the galaxy disk. Long-slit optical spectra (Heckman, Armus, & Miley 1990; Filippenko & Sargent 1992) showed large velocity gradients across the bubble, peaking at $\gtrsim$1500 km s^{-1} relative to galaxy systemic. We (Veilleux et al. 1994) used the HIFI FPS to map radial velocities and [N II]/Hα ratios across the bubble and disk. We concluded that the bubble morphology and kinematics agree quite well with simulations of point energy release in the galaxy ISM. The driving mechanism is uncertain because the AGN is obscured and a nuclear starburst weak enough to be subtle.

We obtained Hα+[N II] and *I*-band images with WFPC2. Figure 1 is a composite of the nuclear region. We used the velocity field and line fluxes from our FP datacube to assign radial velocities to most of the filaments in the WFPC2 image. Bracketing gas motions with two assumed space-velocity fields,

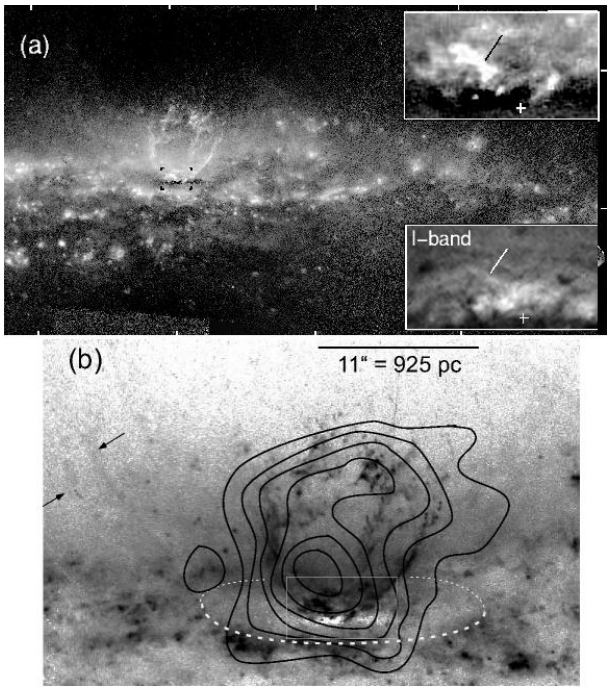

Fig. 1. *HST* (a) Hα+[N II] WPFC2 image of NGC 3079. Ticks every 30″, P.A. 80° at top. The closeup (b) shows that the superbubble is composed of 5 streams of ionized filaments, many resolved in the line-only image. Note also that vertical filaments extend >3 kpc above the disk, and arrows point to those that probably delineate the bubble of shocked wind. The inset panels in (a) show at higher resolution the nuclear region, with the jet-component marked with a tick in both line (top) and *I*-band (bottom) images. Contours in (b) from the *ROSAT* HRI show where the hotter shocked wind mixes with the line-emitting shocked disk gas to cool into the *ROSAT* passband.

we constrained the total momentum and KE of the ionized flow to the range $(0.4-5)\times10^{55}\sqrt{f}$ erg and $(1.6–6)\times10^{47}\sqrt{f}$ dyne s, respectively. f is the gas filling factor, which we constain to be >0.003.

One stream of filaments at the base of the bubble coincides with the axis of the VLBI-scale outflow mapped by Trotter et al. (1998). In Figure 2 we show that the widest emission-line profiles in the superbubble are found along this structure, thereby extending the influence of the jet to 250 pc radius. The bubble is formed from the remaining four filament bundles, which all bend upward to reach the same height then disperse. We could not explain this pattern in terms of a precessing jet, and argued that the wind models cited previously remain the best explanation for the bubble. Despite our better constraint on the gas filling factor, whether an AGN or starburst drives the outflow remains uncertain.

Emission Lines from Jet Flows (Isla Mujeres, Q.R., México, November 13-17, 2000)
Editors: W. J. Henney, W. Steffen, A. C. Raga, & L. Binette

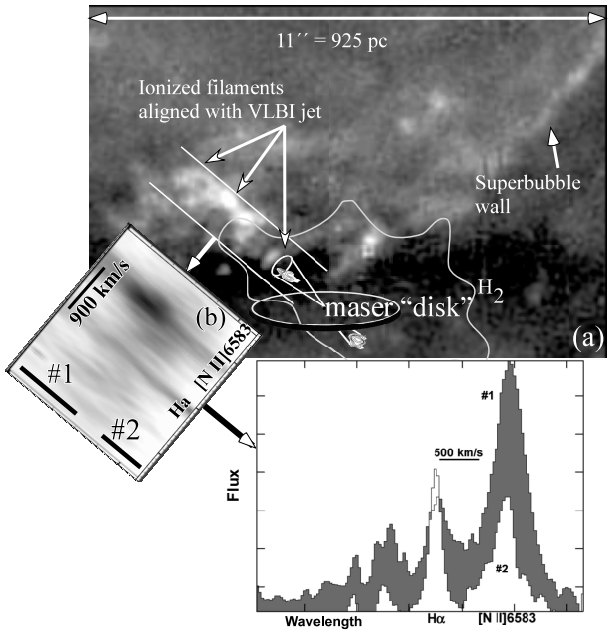

Fig. 2. (a) The base of the superbubble is shown in our *HST* line-only image. The VLBI-scale "maser disk" and jet are shown highly magnified. At much larger scales, (a) shows that a bright filament stream aligns with the jet. Note the space-velocity diagram in (b) and broad spectral line profiles in (c) that we have extracted along the jet from our FP datacube.

3. NGC 4258: THE ACTIVE JET

In NGC 4258 masers are more convincingly distributed in a warped disk, orienting the present outflow. Figure 4 from Cecil et al. (2000) summarizes VLBI/VLBA images of the outflow on the smallest scale, showing that by $\sim 10^4$ AU the jet is collimated and projects almost N/S. We combined new A-configuration data with B- and C-configuration visibilities from the VLA archive to image the radio outflow on larger scales. Figure 5 shows that the near N/S flow ends at a pair of hotspots at $\sim 30''$ radii that straddle the nucleus. The active jet is part of the larger complex of (in)famous "anomalous arms" (van der Kruit, Oort, & Mathewson 1972), which the insert shows are the leading edges of large bubbles.

A spiral galaxy hosts this outflow, so jet/ISM interactions are possible if the flow is close to the galaxy disk plane. In fact, Courtès & Cruvellier (1961) discovered the anomalous arms in visible light, later shown to be line-emitting filaments that in detail are multi-stranded (Ford et al. 1986; Cecil, Wilson, & Tully 1992) and which have optical emission-line flux ratios that are consistent with shock excitation (Cecil, Morse, & Veilleux 1995). We

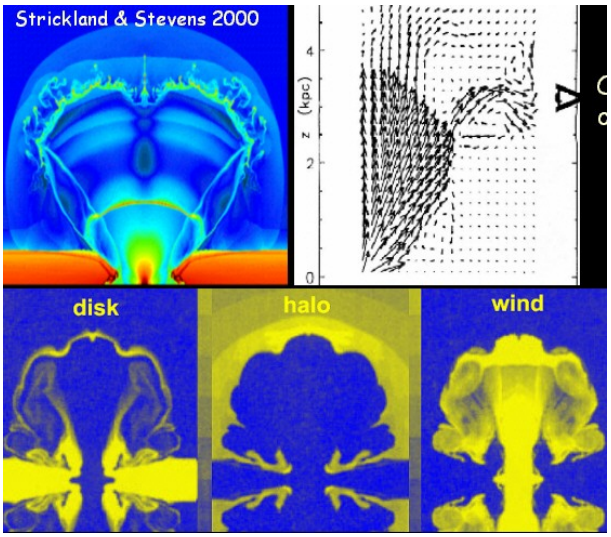

Fig. 3. Snapshots from evolving models of bubbles blown by a nuclear galactic wind, in this case originating from a compact starburst. Top left plots gas pressure from the simulations of Strickland & Stevens (2000) while the rest are from the simulations of Suchkov et al. (1992). The vortical gas flow at top right resembles what we infer from patterns of radial velocities and magnetic fields in the top of the superbubble of NGC 3079.

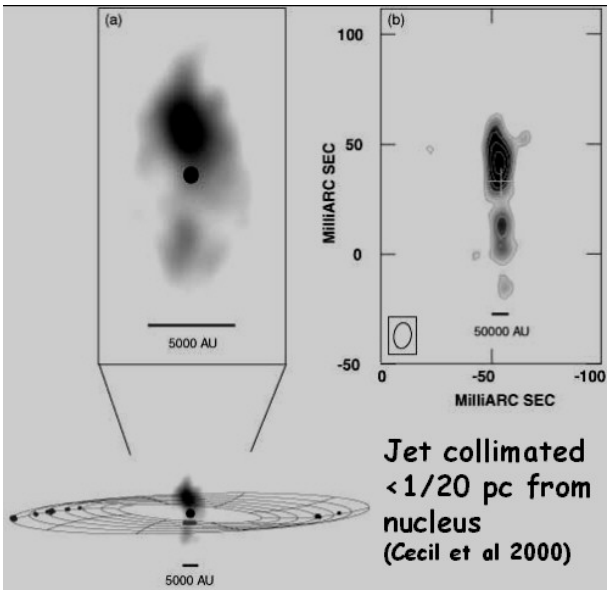

Fig. 4. Near-nuclear emission in NGC 4258, at λ1.3 cm with N at top. (a) VLBI image of the near-nuclear emission in NGC 4258, with a sketch of the warped accretion disk derived from the distribution of H_2O masers shown below. (b) VLBA image of the now collimated jet.

therefore obtained WFPC2 line and continuum images and combined these with a few archival exposures to make the mosaic Figure 7. Now bow

Emission Lines from Jet Flows (Isla Mujeres, Q.R., México, November 13-17, 2000)
Editors: W. J. Henney, W. Steffen, A. C. Raga, & L. Binette

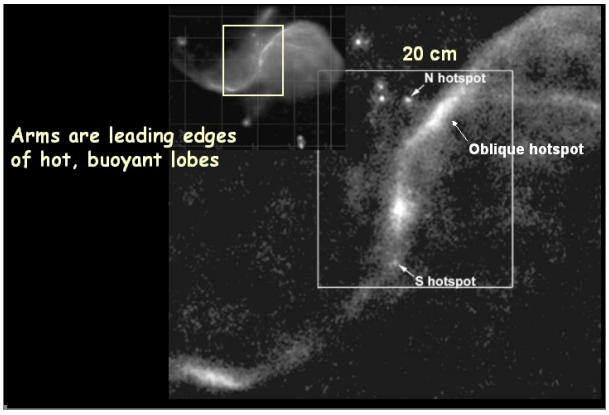

Fig. 5. λ20 cm image of NGC 4258. N at top, extent $3 \times 3'$ with the same region shown in the main panels of Figs. 5 to 7. The inset shows the outflow at larger scale.

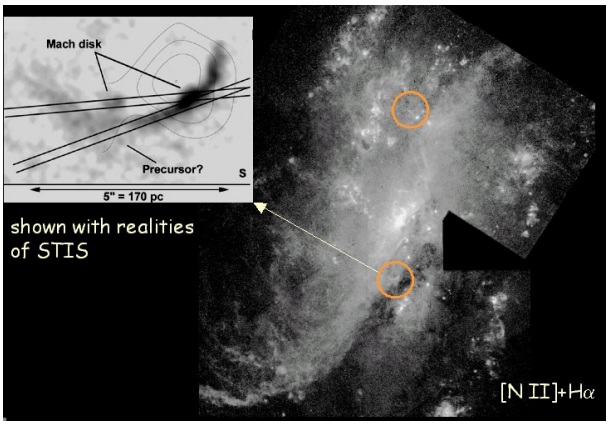

Fig. 6. Log-scaled [N II]+Hα flux image after subtracting starlight. The multi-strand, line-emitting, anomalous arms sweep from lower left to upper right. Two interactions are circled, with the S one detailed in the inset panel. Slits show the practical limits of STIS spectra.

shocks are visible adjacent to both radio hotspots.

Hot gas also concentrates along the arms (Cecil, Wilson, & De Pree 1995), shown clearly in our recently obtained *Chandra X-ray Observatory* (*CXO*) image Figure 7. The N shock complex is visible in this image, and more data to be obtained soon may also uncover the S complex.

We used the ISIS spectrometer at the WHT to obtain 2 Å resolution spectra of the localized interaction sites. Most of the N emission complex is straight enough to stuff through a single 1.″2-wide slit; the S complex required two steps. Figure 8 shows that both complexes emit gas that is blue-shifted (N) or red-shifted (S) by up to 550 km s^{-1} from the ambient velocity at that point in the galaxy. The spectra for the S complex show large differences between the flux distributions of the Hα+[N II] line profiles and

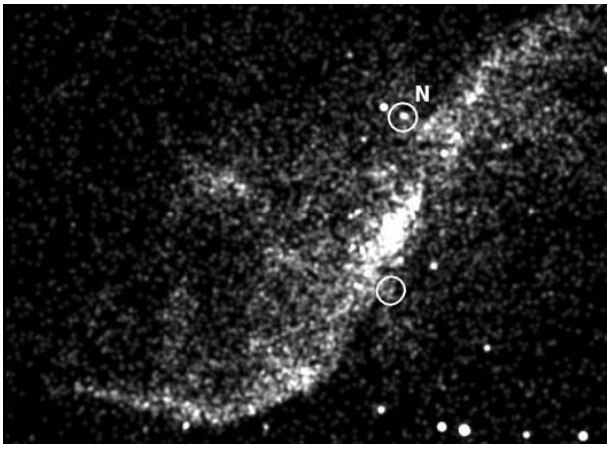

Fig. 7. 14 ksec integration with the ACIS instrument on *CXO*. Data binned and smoothed to 2″ resolution. The positions of the optical N and S shock complexes are circled; the N complex is detected.

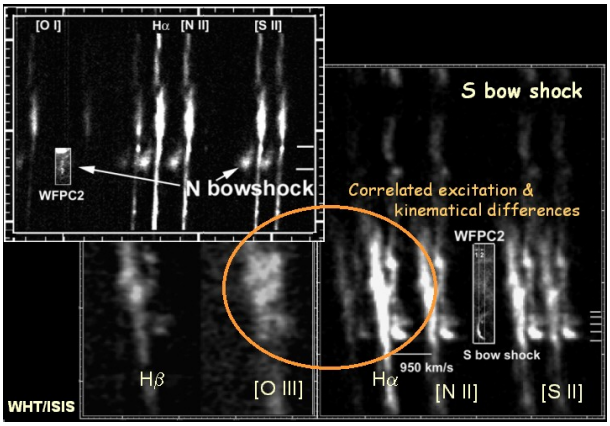

Fig. 8. Long-slit spectra, with the S (main figure) and N (inset) shock complexes shown relative to the structures in the WFPC2 images. Note the large velocity shifts of the complexes relative to the ambient gas, which are well reproduced by the bow shocks modeled in Figure 9.

that of [O III]. This is expected when a bow-shock is resolved. With the structure well-resolved spatially and spectrally, we could fit models similar to those we developed for our earlier program on bow-shocks in Galactic Herbig-Haro objects (Morse et al. 1993, for example). Figure 9 shows that such a model fits only if the apex of the bow structure is at rest in the galaxy ISM, i.e. that both the N and S shocks have stalled with gas now observed to backflow from the working surfaces.

The jet stalls when the driving pressure is reduced. This would arise through a fluctuation of the source mechanical luminosity, or if the jet encounters an unusually dense obstruction. The different orientation of the jet at the VLBI-scale (∼65° from the galaxy disk) favors the second scenario. Figure 10

Emission Lines from Jet Flows (Isla Mujeres, Q.R., México, November 13-17, 2000)
Editors: W. J. Henney, W. Steffen, A. C. Raga, & L. Binette

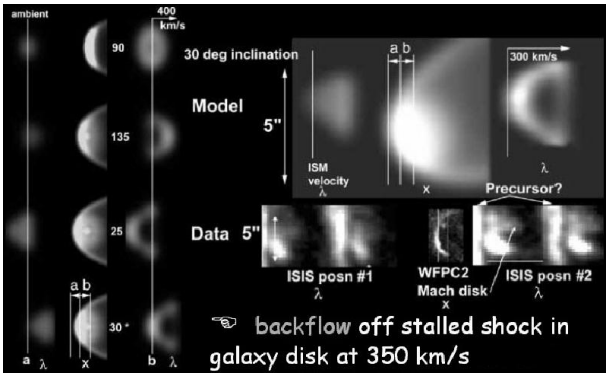

Fig. 9. Appropriate planar shock models are painted onto the 3d surface inferred from the *HST* image, then sliced along two lines shown by "long-slits" to compare with observed spectra. Various orientations and velocity flows are in the left columns, with best-fit to data attained at bottom left. This model implies a stalled bow shock, with backflow at 350 km s^{-1} .

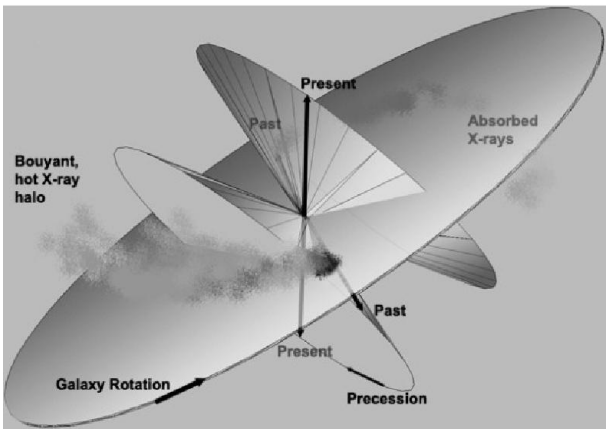

Fig. 10. Precession model for the active jet in NGC 4258. Optical emission arises only when the jet passes through dense gas in the galaxy disk.

shows how precession of the jet source angle ties the two orientations together, with bow shocks appearing only when the outflow intersects the dense galaxy disk. The anomalous arms are bouyant relics of this interaction, trailing because of galactic rotation.

4. NGC 1068: BULLETS OVER BROAD LINES

The narrow-line region (NLR) of NGC 1068 was first resolved spatially by Walker (1969). Subsequent studies used long-slits to map [O III] 5007 Å emission-line profiles, thence to decompose the complex profiles into numerous kinematical subsystems. The NLR is bounded by radio lobes, and contains a radio jet (Wilson & Ulvestad 1987) which exhibits several twists and turns at bright knots in *HST* images (Gallimore, Baum, & O'Dea 1996). *HST* FOS spectroscopy showed that the clouds are photoionized (Kraemer, Ruiz, & Crenshaw 1998) by direct and scattered nuclear radiation in the NE ionization cone, and most recently STIS GTO spectra have shown (Kraemer & Crenshaw 2000, hereafter KC) that line centroids trend to the blue as the ionization potential of the line increases to 1 keV (Figure 11). Because the nucleus is obscured at optical/UV wavelengths, this last result is obtained near the "continuum hotspot" with substantial scattered nuclear light a few tenths of an arcsecond (15 pc) to the NE.

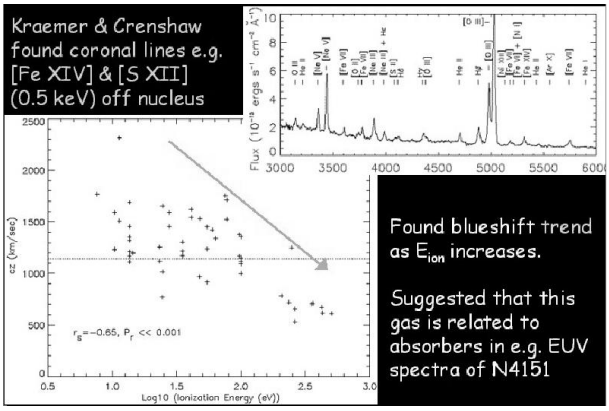

Fig. 11. Trends in the centroid velocity versus ionization potential of emission lines near the nucleus of NGC 1068 (KC). Coronal lines are most blue-shifted relative to galaxy systemic.

The complex spatio-kinematic variations require detailed spectral maps to isolate and characterize the various dynamical subsystems. So we split 14 orbits of STIS spectroscopy evenly between M-grating spectral mapping of the [O III] 5007 Å & Hβ line profiles and less extensive L-grating spectral maps in the far and near UV. We used the 0.″2-wide slit as a reasonable compromise between resolution and mapping efficiency. We obtained 7 parallel slits aligned—because of guide-star constraints—more or less along the axis of the large-scale radio jet. We find that the [O III] 5007 Å and Hβ profiles are very similar, and that there are kinematic components that extend to velocities that exceed the 2900 km s^{-1} separation of the O III doublet. To obtain clean profiles and [O III] 5007 Å/Hβ images for analysis, we therefore parameterized each line with up to 20 Gaussians and constrained the interline fits to have the correct quantum ratio for the doublet. We synthesized the [O III] 5007 Å image from the datacube and registered it to the FOC image (kindly provided by A. Capetti). We used both astrometric registrations (Gallimore et al. 1996; Capetti, Macchetto, & Lattanzi 1997) between radio and optical data to study the jet/ISM interactions; they differ by ∼0.″25.

Emission Lines from Jet Flows (Isla Mujeres, Q.R., México, November 13-17, 2000)
Editors: W. J. Henney, W. Steffen, A. C. Raga, & L. Binette

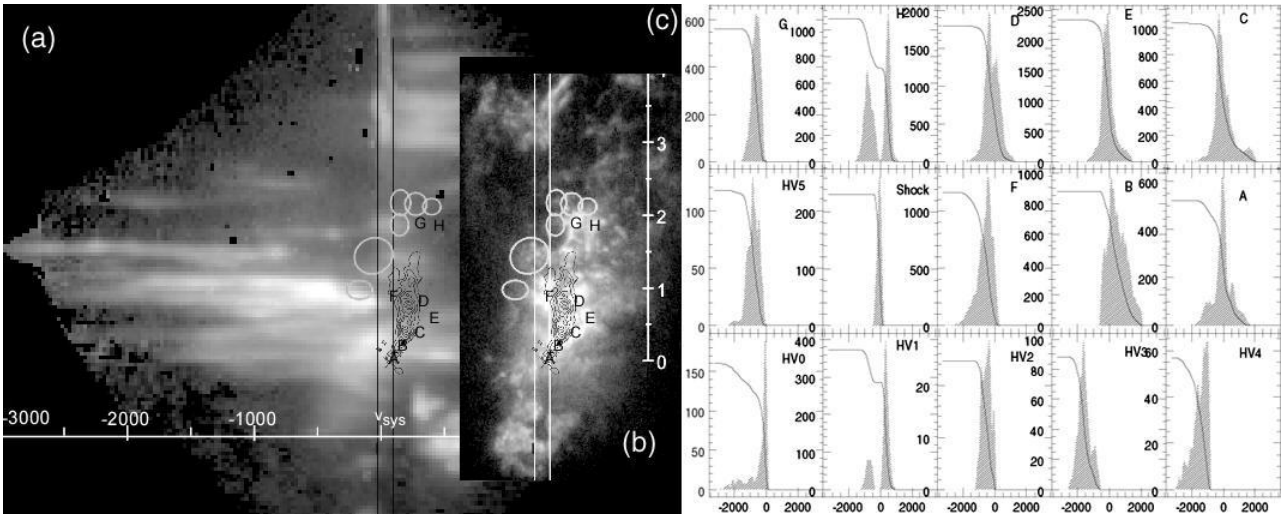

Fig. 12. (a) Log-scaled composite [O III] emission line profiles along one spectrum through the NLR of NGC 1068 are registered in (b) to the FOC [O III] image and the brightest radio contours; spectrum (a) was extracted along the slice shown. The base of the NE radio lobe is at the top of (a) and (b), and the vertical scale is in arc-seconds from the nucleus. Radial velocities exceed 3100 km s^{-1} relative to the galaxy systemic velocity at the circled knots. (c) Kinematic components resolved by our STIS spectra, then summed across the NLR. Velocities are relative to the systemic value and the same arbitrary flux scale is used for all profiles.

We find that the highest-velocity features are barely resolved knots in the FOC line image. Circled in Figure 12b, they are adjacent spectrally to brighter clouds which are blueshifted by several hundred km s^{-1} from the local galaxy rotation curve. The brighter clouds have highest velocity nearest the radio jet, suggesting that the jet has indeed pushed them aside. In this scenario, the high-velocity knots would be ablated from massive molecular clouds in the galaxy disk that have rotated into the jet beam. The high-velocity filaments are all blueshifted because this orientation to us, assuming outflow, has them moving predominantly away from and above the galaxy disk. Similar clumps below the jet would sink into the denser galaxy disk where they would be subject to stronger drag forces hence decelerated more effectively (consistent with the results of Pécontal et al. 1997). If the knots are matter-bounded then they should be more prominent in the line profiles of higher ionization species, thereby blueshifting the line centroids as KC found.

Figure 12c shows the different kinematic components that we have extracted from the STIS datacube. The new high-velocity features are denoted HVx in the bottom rows of Figure 12c and in Table 1, and emit a few percent of the total NLR Hβ flux; properties of the previously identified clouds A−H are also tabulated for comparison. If these clumps were instead viewed projected on the background nuclear continuum source, they would resemble in their kinematics the "warm absorbers" seen in the UV spectra of some Seyferts and the Associated Absorption Line systems seen in a few percent of quasars. While such systems are normally thought to lie much closer to the nucleus than the 100–150 pc projected

TABLE 1

IONIZED CLOUDS IN THE NLR OF NGC 1068

Name	[O III][a] / Hβ	log KE (erg/$n_{e,4}$)[b]	log momentum (dyne s/$n_{e,4}$)[b]
A	15	51.5	43.9
B	16	52.2	44.5
C	16	51.8	44.2
D	18	51.8	44.4
E	17	51.8	44.4
F	18	52.3	44.7
G	22	51.6	44.0
H	14	51.8	44.3
HV0	14	51.0	43.1
HV1	19	52.0	44.3
HV2	16	50.5	43.0
HV3	10	51.5	43.6
HV4	23	51.4	43.4

[a]Dereddened by $E_{B-V} = 0.20 \pm 0.02$ (KC).

[b]Scaled by gas density in units of 10^4 cm^{-3}, and a lower limit assuming that the observed radial velocities are the full space velocities.

radius of the clumps in NGC 1068 (Kraemer et al. 2001, get radii of < 1 pc from photoionization models of the coronal component in NGC 4151). de Kool et al. (2001) established that some of the absorbers in a BALQSO must be ~ 500 pc from that nucleus.

High-velocity features also appear in STIS M-grating spectra of NGC 4151 (Hutchings et al. 1999), although not clearly connected to more massive clouds as in NGC 1068. The clumps in NGC 1068 should be studied in more detail and in higher ionization lines with STIS UV echelle spectra, and especially the higher efficiency of the upcoming *Cosmic Origins Spectrograph* (COS) on *HST*. COS has no spatial resolution so STIS maps must guide it.

A major question is how these clumps survive to such large velocities. Hydro simulations confirm analytic scalings that Rayleigh-Taylor instabilities grow much faster than the cloud is ram accelerated. So clouds shatter before they move more than a few timestheir diameter. While a wind can push the massive reservoirs up to their observed deviations of a few hundred km s^{-1} radial velocities, we are reconsidering radiative acceleration of the photoionized high-velocity clumps. As Dopita (2002) discusses in these proceedings, this approach is also motivated by considerations of the ionization parameters of the high-velocity clumps and incorporates the effects of dust.

5. SUMMARY

We are using ground-based 3d spectrometers to locate energetic hydro structures in AGN outflows. Gas filling factors scale the ionized mass, KE, and momenta of the flows, but are effectively constrained by recombination fluxes when *HST* imaging resolves filaments. So far we have imaged several systems with WPFC2, and (more slowly) mapped the brightest one spectrally by stepping the STIS slit. However, exploiting the spatial resolution to advance understanding of AGN dynamics requires an unfeasibly large time allocation with STIS. Optical diagnostics will come soon from integral-field spectrometers on 8m+ telescopes. Where reddening is small enough to permit UV spectroscopy, STIS will pave the way for detailed studies with the more efficient COS instrument.

Grants GO-6563, GO-6674, and GO-7353 from STScI support this work.

REFERENCES

Capetti, A., Macchetto, F. D., & Lattanzi, M. G. 1997, ApSS, 248, 245
Cecil, G. 2000a, in ASP Conf. Ser. Vol. 195, 3D Spectroscopy in Astronomy, eds. J. Bland-Hawthorn & W. van Breugel (San Francisco: ASP), 263
Cecil, G., et al. 2000, ApJ, 536, 675
Cecil, G., Morse, J. A., & Veilleux, S. 1995, ApJ, 452, 613
Cecil, G., Wilson, A. S., & De Pree, C. 1995, ApJ, 440, 181
Cecil, G., Wilson, A. S., & Tully, R. B. 1992, ApJ, 390, 365
Courtès, G. & Cruvellier, P. 1961, Comp. Rend. Acad. Sci. Paris, 253, 218
de Kool, M., et al. 2001, ApJ, 458, 609
Dopita, M. A. 2002, RevMexAA(SC), 13, 177 (this volume)
Duric, N., & Seaquist, R. S. 1988, ApJ, 326, 574
Filippenko, A. V. & Sargent, W. 1992, AJ, 103, 1
Ford, H. C., et al. 1986, ApJ, 311, L7
Gallimore, J. F., Baum, S. A., & O'Dea, C. P. 1996, ApJ, 464, 198
Heckman, T. M., Armus, L., & Miley, G. K. 1990, ApJS, 74, 833
Hutchings, J., et al. 1999, AJ, 118, 2101
Kraemer, S. B., et al. 2001, ApJ in press (astro-ph/0101037)
Kraemer, S. B., & Crenshaw, D. M. 2000, ApJ, 532, 256 (KC)
Kraemer, S. B., Ruiz, J. R., & Crenshaw, D. M. 1998, ApJ, 508, 232
Morse, J. A., et al. 1993, ApJ, 410, 764
Pécontal, E., et al. 1997, Ap&SS, 248, 167
Strickland, D. K. & Stevens, I. R. 2000, MNRAS, 314, 511
Trotter, A. et al. 1998, ApJ, 495, 470
van der Kruit, P. C., Oort, J. H., & Mathewson, D. S. 1972, A&A, 21, 169
Veilleux, S. et al. 2002, RevMexAA(SC), 13, 222 (this volume)
Veilleux, S. et al. 1994, ApJ, 433, 48
Walker, M. F. 1969, ApJ, 151, 71
Wilson, A. S., & Ulvestad, J. 1987, ApJ, 319, 105

G. Cecil: Dept. of Physics & Astronomy, U. of North Carolina, Chapel Hill, NC 27599 (gerald@thececils.org).
P. Ferruit: Observatoire de Lyon, Saint-Genis Laval Cedex, F-69561, France (pierre@typhon.univ-lyon1.fr).
S. Veilleux: Astronomy Department, U. of Maryland, College Park, MD 20742 (veilleux@astro.umd.edu).

Emission Lines from Jet Flows (Isla Mujeres, Q.R., México, November 13-17, 2000)
Editors: W. J. Henney, W. Steffen, A. C. Raga, & L. Binette